

SpatialDreamer: Incentivizing Spatial Reasoning via Active Mental Imagery

Meng Cao^{1*}, Xingyu Li^{1*}, Xue Liu¹, Ian Reid¹, Xiaodan Liang^{1,2†}

¹Mohamed bin Zayed University of Artificial Intelligence ²Sun Yat-sen University

*Authors contributed equally to this research. †Corresponding author.

<https://github.com/mengcaopku/SpatialDreamer>

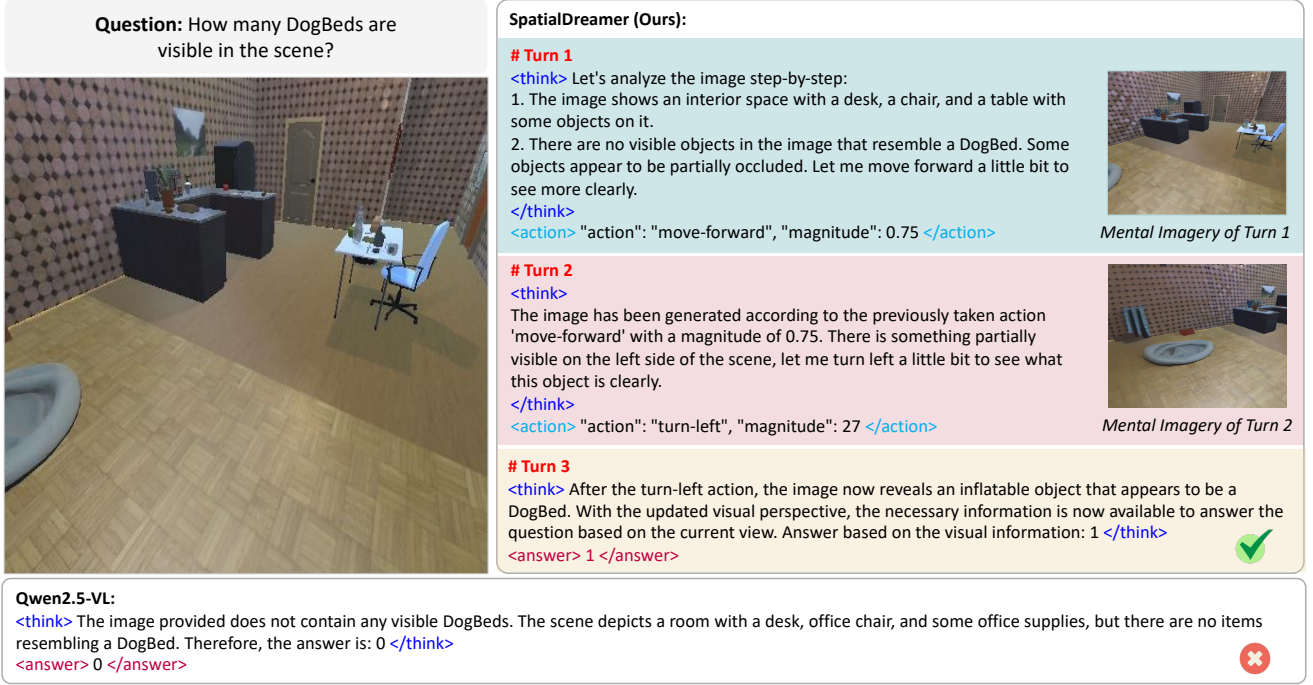


Figure 1. **Case studies of spatial reasoning tasks requiring mental simulation.** Qwen2.5-VL [3] fails to identify occluded objects due to its static single-view perception. Our SpatialDreamer incrementally explores the scene through *active imagination*, invoking world models [84] to generate novel ego-centric views, and integrating the visual evidence into reasoning.

Abstract

Despite advancements in Multi-modal Large Language Models (MLLMs) for scene understanding, their performance on complex spatial reasoning tasks requiring mental simulation remains significantly limited. Current methods often rely on passive observation of spatial data, failing to internalize an active mental imagery process. To bridge this gap, we propose **SpatialDreamer**, a reinforcement learning framework that enables spatial reasoning through a closed-loop process of active exploration, visual imagination via a world model, and evidence-grounded reasoning. To address the lack of fine-grained reward supervision in long-horizon reasoning tasks, we propose **Geometric Policy Optimization (GeoPO)**, which introduces tree-structured

sampling and step-level reward estimation with geometric consistency constraints. Extensive experiments demonstrate that **SpatialDreamer** delivers highly competitive results across multiple challenging benchmarks, signifying a critical advancement in human-like active spatial mental simulation for MLLMs.

1. Introduction

Humans perceive and reason within a three-dimensional world, effortlessly understanding spatial structure, predicting object interactions, and mentally simulating how actions unfold in dynamic physical environments [21, 43]. Recently, Multi-modal Large Language Models (MLLMs) [1, 3, 45] have demonstrated impressive capabilities in gen-

eral scene understanding and even some simple spatial reasoning tasks, *e.g.*, object counting and spatial relation reasoning [8, 62]. However, they remain fragile when confronted with complex spatial reasoning tasks requiring *mental simulation* [50, 67, 79], which refer to the reasoning processes that demand the prediction of spatial or physical outcomes under hypothetical actions or perspective-taking, rather than direct perception of static scenes. For example, in Figure 1, actively shifting the ego-centric perspective is required to answer correctly, whereas relying on a single viewpoint is prone to partial observation and leads to incorrect answers. On the spatial mental modeling benchmark MindCube [67], even the leading proprietary model GPT-4o [45] achieves only 38.81% overall accuracy, barely above random guessing. This underscores the notable inadequacy of current MLLMs in handling such tasks.

Existing approaches attempt to mitigate this deficiency through spatial-aware instruction tuning [9, 16, 27, 37, 74, 81], by exposing MLLMs to synthetic or reconstructed 3D scenes under spatial supervisions such as object layouts and viewpoint relationships. Although straightforward, such methods *passively* observe labeled spatial relations rather than *actively imagining, moving, and updating their internal representation*, as humans naturally do. The recent work MindJourney [63] takes a promising step toward this goal by coupling a frozen MLLM with a controllable world model [84] to simulate novel egocentric views. However, as a test-time scaling approach [56], it lacks a learnable exploration policy and therefore fails to internalize the spatial mental imagery capability within MLLMs. In addition, it is heavily reliant on manually-configured hyper-parameters, *e.g.*, the exploration depth and threshold settings.

To this end, we propose **SpatialDreamer**, a reinforcement learning (RL) framework that mimics human-like, iterative spatial mental reasoning through geometry-aware imagination and interleaved spatial reasoning. Specifically, our SpatialDreamer operates through a closed loop of exploration, imagination, and reasoning. The model sequentially 1) reasons about the scene to select an egocentric action with arguments (*e.g.*, move-forward by 0.75m), 2) invokes world models [84] to generate imagined views simulating the action’s consequence, and 3) integrates the accumulated visual evidence to generate the final answer. Through this iterative process, our SpatialDreamer evolves from the prevalent passive observation to active goal-directed imagination, autonomously learning where to explore, what to observe, and how to reason within its own internal 3D environment.

A key challenge in training such a long-horizontal reasoning framework lies in designing an effective reward structure. As shown in Figure 2 (left), standard RL approaches [23, 68, 70] typically sample multiple independent trajectories for each query and assign *episode-level* re-

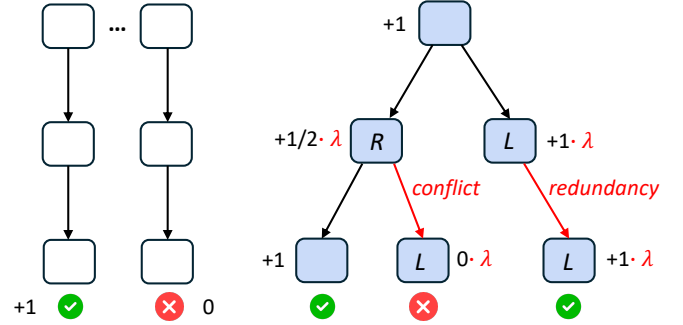


Figure 2. **Conceptual comparisons between (left) vanilla GRPO and (right) our GeoPO.** GRPO samples multiple independent trajectories and relies solely on episode-level rewards. In contrast, our GeoPO achieves step-level reward guidance through a tree-structured sampling scheme with geometric conflict and redundancy detection (identical or opposing actions between adjacent steps). λ is the penalty coefficient. R and L denote the action of turning left/right, respectively.

wards solely based on the correctness of the final answer. While conceptually simple, such methods lack *step-level* reward estimation to provide timely feedback, *i.e.*, whether the current imagination action and the corresponding novel ego-centric views contribute to the final answering. To address this, we propose **Geometric Policy Optimization (GeoPO)**, which follows a tree-structured sampling scheme that performs bottom-up credit assignment for each world-model invocation action, while penalizing geometric redundancy and conflicts. For example in Figure 2 (right), if two consecutive actions within the trajectory are executed in identical or opposite directions, we apply a decay coefficient (typically 0.9) to penalize such sub-optimal rollout strategies. By combining episode and step-level rewards, GeoPO achieves fine-grained spatial reasoning supervision and more stable policy convergence. Experimental results demonstrate that our GeoPO not only achieves superior performance but also exhibits faster convergence compared to the vanilla GRPO [23].

In summary, our contributions are in three-folds:

- We present SpatialDreamer, an RL framework that fosters human-like spatial reasoning by leveraging a world-model-based loop of active exploration, imaginative generation, and evidence integration, thereby internalizing spatial mental imagery as an intrinsic skill.
- We propose GeoPO, a tree-structured sampling scheme to facilitate step-level credit assignment and simultaneously penalize geometric conflict or redundancies.
- Extensive experiments have demonstrated that our SpatialDreamer achieves highly competitive performance on multiple spatial reasoning benchmarks, including SAT [50], Mind-Cube [67], and VSI-Bench [62].

2. Related Work

2.1. Spatial Reasoning

Spatial reasoning refers to the cognitive ability to perceive, mentally represent, and reason about the geometric and topological relationships among objects in three-dimensional space [6, 61, 71]. Numerous benchmarks [22, 32, 42, 50, 67, 76, 77] have consistently demonstrated that current MLLMs exhibit significant limitations in this aspect. Therefore, early approaches sought to enhance spatial reasoning through input augmentation, *e.g.*, introducing geometric cues from depth images [5, 9, 14, 40, 49] or point clouds [20, 24, 73]. The recent efforts have shifted towards leveraging RL to incentivize the spatial reasoning capabilities of MLLMs [9, 47, 74]. Pioneering works introduce large-scale datasets such as VSI-100K [37], SPAR-7M [74], and MSMU [9], and employed GRPO training paradigms [23] to encourage spatially-grounded reasoning. To inject geometric priors, VGLLM [81] and VLM3R [16] directly utilize pre-trained 3D foundation models (VGGT [58] and CUT3R [59]) as robust 3D feature extractors to provide rich geometric representations. In a parallel approach, 3DRS [27] and ThinkWith3D [13] adopt a distillation strategy, leveraging VGGT [58] as a teacher model for the efficient transfer of 3D knowledge. However, such methods passively observe spatial annotations, whereas our SpatialDreamer proposes to actively explore and imagine with a world model in constrained views.

2.2. Spatial Mental Imagery

Spatial mental imagery [4, 13, 15, 19, 65] refers to the fundamental cognitive skill of constructing and manipulating mental representations of spatial environments. In contrast to basic spatial reasoning, spatial mental imagery specifically requires the ability to build human-like internal worlds and perform dynamic simulations within them. Evaluation results on mental imagery datasets (*e.g.*, MindCube [67], SAT [50], 3DSRBench [42]) indicate that current MLLMs still lack this crucial high-level reasoning capability. To this end, SAT [50] enhances allocentric reasoning through a dedicated SFT dataset, while the recently proposed APC [32] simulates human mental imagery by constructing coarse 3D scene abstractions and transforming them into the reference viewer’s coordinate frame. Another approach, MindJourney [63], leverages external visual feedback to iteratively improve perspective-taking ability. However, both MindJourney [63] and APC [32] are test-time scaling strategies [56] that involve complex hand-crafted pipelines, without equipping MLLMs with the intrinsic mental imagery capability. Therefore, our SpatialDreamer mimics human-level reasoning by leveraging a world model for active exploration and seamlessly iterating between linguistic and visual reasoning.

2.3. RL for LLM Reasoning

Recent studies have shown that reinforcement learning [23, 28, 48] can substantially enhance the reasoning ability of MLLMs. Early approaches [35, 38, 53, 82] relied on reward models to provide supervision at the outcome or process level. However, training reward models requires large amounts of high-quality annotated data and tends to suffer from reward hacking [55] as RL training progresses. More recently, rule-based RL frameworks such as GRPO [23] and its variants (DAPO [68], VAPO [70]) have demonstrated strong scalability and efficiency, yet they typically offer only trajectory-level reward signals, lacking fine-grained process-level feedback. To address this limitation, several studies have proposed tree-structured sampling [25, 26, 36, 64, 66] to explore diverse reasoning branches within a single rollout, yielding denser feedback than plain chain sampling. Building upon this idea, our proposed geometric policy optimization adapts tree-structured RL to the geometric mental imagery setting by constructing per-step dense rewards while simultaneously accounting for geometric redundancy and conflicts across steps, thus driving the generation of optimal and efficient action trajectories.

3. Methodology

We firstly present preliminaries including the overview and structured reasoning pattern of our SpatialDreamer in Sec. 3.1. Then we detail the geometric policy optimization in Sec. 3.2. Finally, we discuss the construction process of our SpatialDreamer-SFT dataset in Sec. 3.3.

3.1. Preliminaries

Overview. As shown in Figure 3a, our SpatialDreamer follows an agentic RL framework featuring multi-round interactive reasoning that combines egocentric imagination from external world models with answer generation.

Given the input question q and image v , the overall reasoning process can be decomposed as follows:

$$\underbrace{\prod_{\leq T_{\max}} \pi_{\theta}(a \mid q, v)}_{\text{active mental imagery}} \cdot \underbrace{\pi_{\theta}(o \mid q, v, e)}_{\text{answer gen}}, \quad (1)$$

where T_{\max} is the maximum iteration number. o is the output responses. a denotes the action rollouts (*e.g.*, *forward 1m*), which are fed into a world model \mathbf{W} (implemented as SVC [84]) to generate the novel ego-centric views e :

$$e = \mathbf{W}(v, a). \quad (2)$$

Structured Reasoning. In each round of active mental imagery, the cognitive process comprises the analytical thinking tokens encapsulated within `<think>` and `</think>` tags and *mental imagination* tokens delimited by `<imagine>` and `</imagine>` tags. Specifically, the

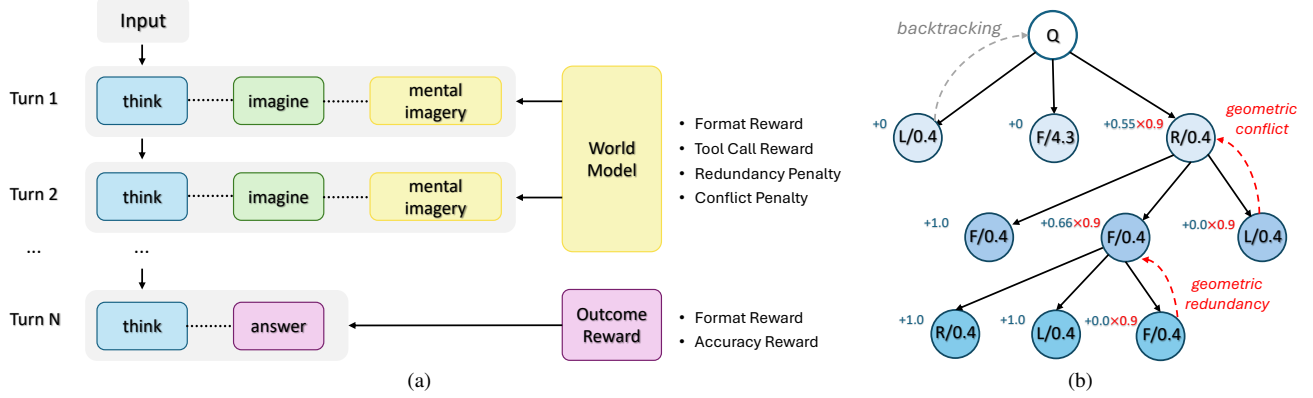


Figure 3. (a) **An overview of SpatialDreamer.** In each round, SpatialDreamer **thinks** about the geometric context and **imagines** novel ego-centric views by invoking a world model using the rollout parameters (*e.g.*, left-27m), and finally **answers** by integrating all the accumulated evidence. (b) **The architecture of GeoPO.** Starting from the question, at most N trajectories are generated in each step until the answer is generated or the maximum depth limit T_{\max} is reached. The reward for a **leaf node** is computed based on the ground-truth answer, while the reward for any **intermediate node** is defined as the average of the rewards of all its direct child nodes. Additionally, a **geometric penalty** coefficient (*i.e.*, 0.9) is imposed on sub-optimal rollouts including redundant or conflicting actions. “L/0.4” denotes turning left by 0.4 m, and other symbols follow the same convention. The values on the left of each node indicate the step-wise rewards.

mental imagination tokens are selected from the primitive action space:

$$\mathbb{A} = \{\text{forward } d, \text{ left } \theta_l, \text{ right } \theta_r\}, \quad (3)$$

where d specifies the moving distance (meters), while θ_l and θ_r describe the rotational angles of left and right turns, respectively, in degrees.

Once sufficient external information has been acquired or the maximum iteration step T_{\max} is reached, the model generates the final responses composed of thinking tokens (within `<think>` and `</think>`) and answer tokens (within `<answer>` and `</answer>`).

3.2. Geometric Policy Optimization

To alleviate the reward sparsity in standard RL, we propose GeoPO, which employs a tree-structured sampling scheme that utilizes both episode-level and step-level rewards.

Tree-structured Sampling. The entire sampling process is modeled as an N -ary tree with a maximum depth of D . At each decoding step, the model samples N world-model invocations with different control arguments, expanding N new branches from the current node. To encourage reflective reasoning, the tree structure supports a backtracking mechanism, allowing the model to revert to a parent node and regenerate alternative branches when necessary.

Reward Design. SpatialDreamer is driven by a hybrid reward integrating episode and step-level signals, alongside a geometric penalty to mitigate sub-optimal action rollouts.

- **Episode-level reward:** This reward combines 1) a format reward, 2) a final answer reward computed against the ground-truth correctness, and 3) a tool-call reward

that encourages each invocation of the world model. We denote the episode reward for the i -th trajectory as r_i^e .

- **Step-level reward:** As shown in Figure 3b, each **leaf node** receives a binary reward, conditioned on whether it generates the correct answer. These rewards are then recursively computed in a bottom-up manner across the tree. Specifically, the reward for any intermediate node is set to the average rewards of all its direct child nodes:

$$r_{i,t}^s = \frac{1}{|\mathcal{C}(i,t)|} \sum_{c \in \mathcal{C}(i,t)} r_c, \quad (4)$$

where $\mathcal{C}(i,t)$ denotes the set of all direct child nodes of the t -th node in the i -th trajectory and $r_{i,t}^s$ represents the corresponding step-wise reward.

- **Geometric penalty:** Since the generated trajectories contain some geometrically suboptimal action sequences, we apply an additional scaling factor as penalty to these nodes: 1) *redundancy*: executing two actions in the same direction (*e.g.*, move left), which could be accomplished by a single action; 2) *conflict*: performing two consecutive actions in opposite directions (*e.g.*, move left followed by move right). Accordingly, we impose a reward coefficient $\lambda = 0.9$ on such nodes falling into these two cases as a geometric penalty.

Thus, the overall reward is as follows:

$$r_{i,t} = r_i^e + \lambda \cdot r_{i,t}^s, \quad (5)$$

where $r_{i,t}$ denotes the final overall reward for the t -th node in the i -th trajectory.

Optimization Objective. Our SpatialDreamer is trained by adapting GRPO [23] to the step-wise optimization version.

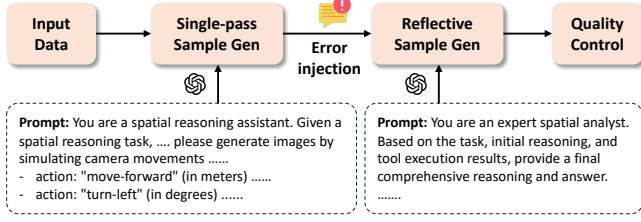


Figure 4. The construction process of SpatialDreamer-SFT dataset including single-pass and reflective reasoning samples. Refer to supplementary materials for more details.

The policy π_θ is then optimized by maximizing the following objective function:

$$\mathcal{J}(\theta) = \mathbb{E}_{\mathbf{q}, \mathbf{v}, \{\mathbf{o}_i\}_{i=1}^G \sim \pi_{\theta_{\text{old}}}} \left[\frac{1}{G} \sum_{i=1}^G \frac{1}{|\mathbf{o}_i|} \sum_{t=1}^{|\mathbf{o}_i|} \min \left(\rho_{i,t}(\theta) A_{i,t}, \text{clip}(\rho_{i,t}(\theta), 1 - \varepsilon, 1 + \varepsilon) A_{i,t} \right) - \beta \mathbb{D}_{\text{KL}}(\pi_\theta \| \pi_{\text{ref}}) \right], \quad (6)$$

where the components in **red** emphasize the step-wise reward design as opposed to the episode-level reward scheme in vanilla GRPO. The importance sampling ratio $\rho_{i,t}(\theta)$ and the advantage $A_{i,j}$ are defined as follow:

$$\rho_{i,t}(\theta) = \frac{\pi_\theta(\mathbf{o}_{i,t} \mid \mathbf{q}, \mathbf{o}_{i,<t})}{\pi_{\theta_{\text{old}}}(\mathbf{o}_{i,t} \mid \mathbf{q}, \mathbf{o}_{i,<t})}, \quad (7)$$

$$A_{i,j} = \frac{r_{i,t} - \text{mean}(\{r_{i,t}\}_{i=1, t=1}^G, |\mathbf{o}_i|)}{\text{std}(\{r_{i,t}\}_{i=1, t=1}^G, |\mathbf{o}_i|)}. \quad (8)$$

3.3. SpatialDreamer-SFT Dataset

To endow MLLMs with preliminary agentic imagination behaviors, we construct the SpatialDreamer-SFT dataset to elicit the think–imagine–answer reasoning pattern. Specifically, the videos are sourced from the training set of MindCube [67], and the curated data consists of both single-pass reasoning samples and reflective reasoning samples (*cf.* Figure 4). Refer to the supplementary material for detailed statistical information.

Single-pass reasoning samples. These samples are curated to demonstrate monotonic, one-pass analytical and geometric reasoning without subsequent correction. The data is produced by prompting a frozen, high-capacity teacher model Qwen3-VL-235B-A22B-Instruct.

Reflective reasoning samples. During the above data construction process, we observe that few samples naturally exhibit reflective thinking, *i.e.* explicitly including error recognition, backtracking, and self-correction behaviors. This scarcity likely stems from the limited native agentic reasoning capabilities of current MLLMs. To address this, we pro-

pose an *error injection* strategy in Figure 4, which intentionally injects a tool-call action with the incorrect argument at an intermediate point of the trajectory and prompt the teacher model to simulate an “*error–reflection–correction*” scenario. Typically, only one or two erroneous steps are introduced to maintain the recoverability and overall coherence of the reasoning chain.

Quality Control. As highlighted by previous studies, the quality of the SFT dataset is more critical than its scale [72, 80, 83]. We therefore conduct a rigorous manual quality inspection on both the generated reasoning traces and the world-model–produced novel ego-centric views: 1) *logical consistency*: Experts manually verify the format, coherence, and plausibility of each reasoning step within a trace, ensuring that it follows a valid and interpretable logical progression; 2) *geometric plausibility*: For the generated novel views, we inspect their geometric consistency with the corresponding action instructions and confirm the absence of obvious rendering artifacts; 3) *goal relevance*: Each reasoning trace is further checked to ensure that it meaningfully contributes to accomplishing the given task rather than producing redundant or irrelevant reasoning.

4. Experiment

4.1. Experimental Settings

Dataset and Benchmarks. To demonstrate the consistent effectiveness, we conduct experiments on both spatial mental modeling and general spatial reasoning datasets:

- **Spatial mental modeling datasets:** These datasets focus on dynamic spatial reasoning, requiring ego-motion or mental simulation: 1) **SAT** [50]: The test split comprises SAT-Synthesized with 4,000 synthetic questions rendered in AI2-THOR [31] indoor scenes, and SAT-Real with real images spanning indoor and outdoor environments. The training set contains 175K questions across 22K procedurally generated scenes, covering egocentric movement, object movement, allocentric perspective, goal aiming, and action consequences; 2) **MindCube** [67]: This dataset is designed for evaluating and training spatial mental modeling capabilities. The evaluation set (MindCube-Tiny) includes 21,154 questions and 3,268 images organized into 976 multi-view groups, while the training set comprises 10,000 reasoning chains and 10,000 ground truth cognitive maps.
- **General spatial reasoning dataset:** We evaluate on the VSI-Bench [62] dataset, which assesses general spatial reasoning capabilities, including object counting, relative direction, *etc.* Following VGLLM [81], we sample 234K samples from SPAR-7M [74] and 63K samples from LLaVA-Hound [78] as the training dataset.

Implementation Details. For SFT, we conduct the full-parameter training for three epochs using the AdamW op-

Table 1. **Comparisons results on SAT dataset** including the real-world and synthesized splits. MindJourney (o1, SVC/SWM) [63] denotes variants implemented based on OpenAI o1 [28] with SVC [84] or SWM [63] models. The top-1 and top-2 accuracies are denoted by the **red** and underlined values, respectively.

Method	SAT-Real						SAT-Synthesized					
	EgoM	ObjM	EgoAct	Goal	Pers	AVG	EgoM	ObjM	EgoAct	Goal	Pers	AVG
<i>Generalist MLLMs</i>												
GPT-4V [44]	–	–	–	–	–	50.7	54.7	32.7	52.0	50.5	34.2	44.8
Gemini1.5-flash [52]	–	–	–	–	–	57.6	67.1	33.1	52.9	64.0	32.7	50.0
Gemini1.5-pro [52]	–	–	–	–	–	64.8	57.7	29.8	55.5	56.9	49.5	49.9
GPT-4o [45]	56.5	85.0	50.0	64.0	45.0	60.3	64.7	86.8	51.9	68.7	43.4	61.0
GPT-4.1 [46]	95.7	73.9	78.3	88.2	39.4	74.0	75.3	89.0	57.8	78.3	41.5	66.4
o1 [28]	78.3	82.6	73.0	73.5	69.7	74.6	78.0	85.9	65.4	86.0	54.6	72.4
InternVL3-14B [85]	56.5	69.5	54.0	73.5	45.4	59.3	77.6	85.9	53.3	84.5	20.6	61.6
LLaVA-1.5-13B [39]	–	–	–	–	–	41.6	46.6	73.8	49.7	45.6	39.9	51.1
LLaVA-Video-7B [78]	–	–	–	–	–	53.5	56.4	82.7	48.0	52.9	47.1	57.4
<i>Test-time Scaling Methods</i>												
MindJourney (o1, SVC) [63]	100.0	65.2	78.4	82.4	63.7	77.3	87.1	80.4	72.3	89.3	70.1	78.6
MindJourney (o1, SWM) [63]	95.7	82.6	83.8	88.2	75.8	84.7	82.4	80.4	76.6	88.1	60.7	76.8
<i>Spatial MLLMs</i>												
Robopoint-13B [69]	–	–	–	–	–	46.6	50.2	69.4	48.8	72.6	25.5	53.3
SAT (LLaVA-1.5-13B) [10]	–	–	–	–	–	54.9	61.7	90.2	91.4	96.8	98.5	87.7
SAT (LLaVA-Video-7B) [10]	–	–	–	–	–	63.4	79.6	80.4	85.3	56.4	88.4	78.0
Robix-32B [17]	–	–	–	–	–	79.6	–	–	–	–	–	–
SpatialDreamer (Ours)	100	90.5	93.5	92.7	90.3	93.9	95.4	93.1	91.8	94.9	<u>89.8</u>	92.5

Table 2. **Comparison results on MindCube-Tiny dataset.** The results of 3DThinker[†] [13] are reported based on the Qwen2.5-VL-7B [3] backbone. The top-1 and top-2 accuracies are denoted by the **red** and underlined values, respectively.

Method	Overall	Rotation	Among	Around
<i>Generalist MLLMs</i>				
GPT-4o [45]	38.8	32.6	40.2	29.2
Claude-4-Sonnet [2]	44.8	48.4	44.2	47.6
LLaVA-OV-7B [34]	47.4	36.5	48.4	44.1
LLaVA-Video-7B [78]	41.9	35.7	43.6	30.1
LongVA-7B [75]	29.5	35.9	29.6	24.9
InternVL2.5-8B [11]	18.7	36.5	18.2	13.1
Qwen2.5-VL-7B [3]	29.3	38.7	29.5	21.4
DeepSeek-VL2 [41]	47.6	37.0	50.4	26.9
Mantis-8B [30]	41.1	37.6	40.2	51.0
<i>Spatial MLLMs</i>				
Ego3D-VLM [22]	44.4	54.3	65.5	69.5
RoboBrain [29]	37.4	35.8	38.3	29.5
SpatialVLM [8]	22.8	37.7	21.3	29.3
Spatial-MLLM [60]	32.1	38.4	20.9	32.8
Space-Qwen [8]	33.3	38.0	33.7	26.3
3DThinker [†] [13]	76.0	55.0	83.0	76.0
SpatialDreamer (Ours)	84.9	87.5	<u>78.2</u>	93.5

timizer. We adopt a cosine learning rate scheduler with an initial learning rate of 1e-5 and a warmup ratio of 0.1. All experiments are run on 8 NVIDIA A100 GPUs with BF16 precision and a global batch size of 64. For RL, the whole training pipeline is implemented based on the verl frame-

work [54]. We adopt Qwen2.5-VL-7B-Instruct [3] as the baseline MLLM. Stable Virtual Camera [84] is used as the world model, which is deployed for tool-call through the ray engine [51] with 16 A100 GPUs. The maximum tree depth of our GeoPO is set to 3, and the number of child nodes for each node is restricted to fewer than 3. The RL training is conducted with a batch size of 128 and a learning rate of 1e-6 on 8 A100 GPUs.

4.2. Experimental Comparisons

Results on spatial mental modeling datasets. We compare our SpatialDreamer against the following approaches: 1) generalist MLLMs, designed for general-purpose understanding; 2) spatial MLLMs, which typically employ constructed spatial-oriented datasets for instruction tuning; and 3) test-time scaling methods, which enhance model performance by allocating extra compute after training.

As shown in Table 1, SpatialDreamer achieves state-of-the-art performance on SAT benchmark [50] across both the real and synthesized splits. It surpasses all generalist, spatial, and test-time scaling methods by a large margin, reaching an average score of 93.9% on SAT-Real and 92.5% on SAT-Synthesized. For the MindCube-Tiny benchmark [67] in Table 2, our SpatialDreamer also obtains state-of-the-art performance with an overall score of 84.9%. Compared to the baseline of Qwen2.5-VL-7B [3], our model achieves an absolute improvement of 55.6% in overall accuracy (84.9% vs. 29.3%). While slightly trailing 3DThinker [13] in the

Table 3. **Comparison with state-of-the-art models on VSI-Bench.** The top-1 and top-2 accuracies are denoted by the **red** and underlined values, respectively. * denotes the method using additional geometric embeddings [58, 59].

		Obj. Count	Abs. Dist.	Obj. Size	Room Size	Rel. Dist.	Rel. Dir.	Route Plan	Appr. Order
Model	Avg.	Numerical Answer			Multiple-Choice Answer				
Generalist MLLMs									
GPT-4o [45]	34.0	46.2	5.3	43.8	38.2	37.0	41.3	31.5	28.5
Gemini-1.5-Flash [57]	42.1	49.8	30.8	53.5	54.4	37.7	41.0	31.5	37.8
Gemini-1.5-Pro [57]	45.4	56.2	30.9	64.1	43.6	51.3	46.3	36.0	34.6
InternVL2-8B [12]	34.6	23.1	28.7	48.2	39.8	36.7	30.7	29.9	39.6
InternVL2-40B [12]	36.0	34.9	26.9	46.5	31.8	42.1	32.2	34.0	39.6
LLaVA-Next-Video-7B [33]	35.6	48.5	14.0	47.8	24.2	43.5	42.4	34.0	30.6
LLaVA-Next-Video-72B [33]	40.9	48.9	22.8	57.4	35.3	42.4	36.7	35.0	48.6
LLaVA-OV-7B [34]	32.4	47.7	20.2	47.4	12.3	42.5	35.2	29.4	24.4
LLaVA-OV-72B [34]	40.2	43.5	23.9	57.6	37.5	42.5	39.9	32.5	44.6
Qwen2.5-VL-7B [3]	33.0	40.9	14.8	43.4	10.7	38.6	38.5	33.0	29.8
Qwen2.5-VL-72B [3]	37.0	25.1	29.3	54.5	38.8	38.2	37.0	34.0	28.9
Spatial MLLMs									
SPAR-8B [74]	41.1	-	-	-	-	-	-	-	-
VG-LLM-4B [81]	46.1	66.4	36.6	55.2	56.3	40.8	43.4	30.4	39.5
Video-R1-7B [18]	37.1	-	-	-	-	-	-	-	-
vsGRPO-V-7B [37]	40.7	59.9	29.6	50.8	48.3	35.4	35.6	34.0	31.5
SpaceR-7B [47]	45.6	-	-	-	-	-	-	-	-
VGLLM-8B* [18]	50.7	67.9	37.7	58.6	62.0	46.6	40.7	32.4	59.2
VLM-3R-7B* [7]	60.9	70.2	49.4	69.2	67.1	65.4	80.5	45.4	40.1
SpatialDreamer (Ours)	62.2	71.1	48.1	67.0	65.9	67.8	86.4	47.5	37.2

Table 4. **Ablation studies of both SpatialDreamer-SFT data and RL training methods.** “single-pass” and “reflective” represent the two types of SFT data, with the former showing one-pass reasoning and the latter involving reflective thinking (*cf.* Sec. 3.3). “w/o penalty” denotes GeoPO without applying geometric penalty (*cf.* Sec. 3.2).

Exp	SFT Data		RL Method			SAT-Real	SAT-Synth	MindCube	VSI-Bench
	single-pass	reflective	GRPO	GeoPO	w/o penalty	Avg	Avg	Avg	Avg
#1	✓	✓		✓		93.9	92.5	84.9	62.2
#2	✓	✓	✓			85.6	86.9	79.4	59.3
#3	✓	✓			✓	89.2	90.1	83.7	60.5
#4				✓		70.4	71.4	48.9	57.8
#5	✓			✓		85.2	86.1	73.9	59.7
#6		✓		✓		83.8	84.3	71.0	59.3

split of “Among” (83.0% *vs.* 78.2%), our method demonstrates overall superior performance, thereby establishing a new performance frontier for spatial MLLMs. These results demonstrate that our proposed *active mental imagery* mechanism is particularly effective for tasks requiring perspective taking, mental imagination, and dynamic simulation.

Results on general spatial reasoning dataset. As shown in Table 3 on VSI-Bench, our SpatialDreamer demonstrates substantial superiority with the average accuracy reaching 62.2%, outperforming all generalist and spatial MLLMs by a clear margin. Notably, SpatialDreamer excels in sub-tasks of object counting (+0.9%), relative distance (+2.4%), rel-

ative direction (+5.9%), and route planning (+2.1%), indicating that these categories require MLLMs to engage in active mental imagery and multi-perspective reasoning for more comprehensive spatial understanding. In addition, our SpatialDreamer also outperforms advanced spatial MLLMs such as VLM-3R and VGLLM, even though these models employ explicit geometric embeddings for training [58, 59].

4.3. Ablation Studies

GRPO *vs.* Our GeoPO. We conduct comparisons between the standard GRPO and our proposed GeoPO to validate the efficacy of our tree-structured sampling scheme with hybrid

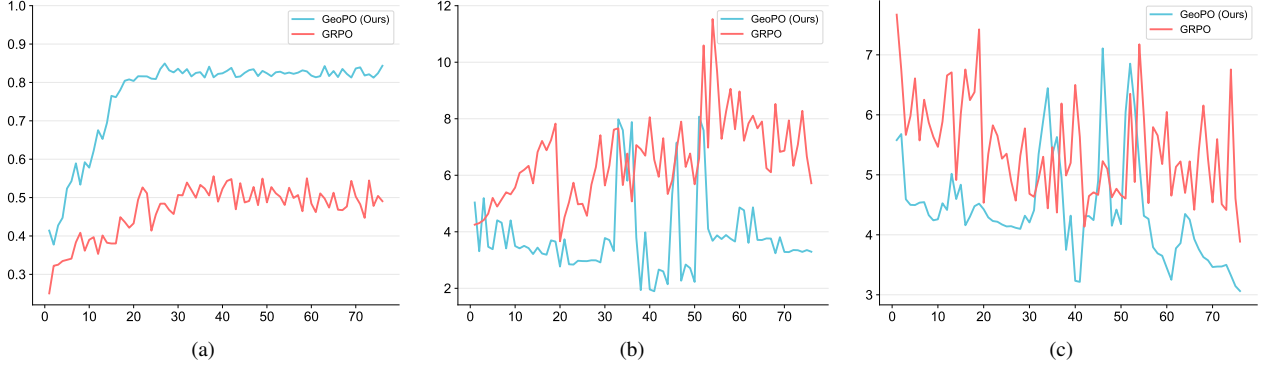


Figure 5. **Efficiency analysis** between GRPO and GeoPO. (a) Reward curve along training steps. (b) Per-trajectory generation time (s): the average time required to generate one trajectory; (c) Per-token generation time (ms): the average time required to generate one token.

rewards. As quantified in Table 4, GeoPO achieves the consistent improvement compared to GRPO (*cf.* Exp #1 vs. Exp #2). For instance, on MindCube-Tiny [67], our GeoPO outperforms GRPO by an absolute value of 5.5% in average accuracy. These results substantiate the necessity of step-wise reward signals, which effectively mitigate the reward sparsity inherent in standard RL frameworks and provide dense supervision throughout the action trajectory.

Ablations of geometric penalty. We further investigate the contribution of the proposed geometric penalty in GeoPO. As shown in Table 4, removing the geometric penalty leads to a noticeable performance degradation across all benchmarks (*cf.* Exp #1 vs. Exp #3). For example, the method with the geometric penalty achieves 1.2% higher average accuracy on MindCube-Tiny compared to the one without it. This demonstrates that penalizing conflicting and redundant spatial trajectories effectively regularizes the exploration process, encouraging geometry-consistent reasoning.

Ablations of SFT data. As detailed in Section 3.3, our SpatialDreamer-SFT dataset comprises both single-pass and reflective samples. We conduct an ablation study to evaluate their individual contributions to the performance. As shown in Table 4, using both types (*i.e.*, Exp #1) yields the best overall performance, indicating their complementarity in shaping reasoning behaviors. In contrast, RL training without using SFT data (Exp #4 in Table 4) leads to a significant performance drop, likely because the absence of SFT data deprives the model of exposure to the tool-call reasoning paradigm, making it difficult for MLLMs to learn and internalize this reasoning pattern effectively. Moreover, training with only *single-pass* data surpasses the *reflective*-only variant (*cf.* Exp #5 vs. Exp #6 in Table 4), suggesting that the single-pass reasoning SFT data provide a stronger foundation for agentic RL.

Efficiency analysis of GeoPO. To analyze the efficiency of our proposed GeoPO, we visualize three key indicators to compare it with GRPO: **1) Reward curve:** As shown

in Figure 5a, we provide the reward curves over training steps. Compared with GRPO, our GeoPO exhibits faster convergence and achieves higher reward values, highlighting the effectiveness of incorporating fine-grained step-level reward modeling; **2) Per-trajectory generation time:** We measure the average generation time per trajectory along training steps. As illustrated in Figure 5b, our GeoPO requires less trajectory generation time than GRPO across almost all training steps, owing to its tree-structured design that allows prefix sharing among trajectories, leading to substantial efficiency gains; **3) Per-token generation time:** We further record the average generation time per token, which directly reflects the runtime efficiency of different RL methods. As shown in Figure 5c, GeoPO consistently achieves lower per-token generation latency than GRPO during most of the training stage. In summary, our GeoPO strikes a superior balance between convergence efficiency and policy effectiveness, providing both faster convergence and higher performance.

5. Conclusion and Future Works

In this work, we introduced SpatialDreamer, an RL framework that endows MLLMs with human-like active spatial mental simulation capabilities. Specifically, our spatial-Dreamer reasons about the scene and invokes a world model to generate novel ego-centric views that in turn, assist the evidence-grounded reasoning. To address the sparse reward challenges, we further proposed GeoPO, a geometric policy optimization scheme that leverages tree-structured sampling and step-level reward estimation with geometric consistency constraints. Extensive experiments across diverse benchmarks demonstrate that SpatialDreamer not only achieves superior performance, but also obtains faster convergence compared to vanilla RL methods. In future work, we aim to internalize the world-model-based imagination capability into MLLMs, enabling unified spatial reasoning and generative perception.

6. Appendix

To supplement the findings presented in the main paper, this supplementary material offers additional quantitative and qualitative results. The specific contents are as follows:

- Statistics of SpatialDreamer-SFT dataset.
- Visualizations of response length.
- Prompts for SpatialDreamer-SFT Curation.
- Evaluation prompts.
- Qualitative results of SpatialDreamer.

Statistics of SpatialDreamer-SFT dataset. Table 5 summarizes the key statistics of the SpatialDreamer-SFT dataset. It contains two types of samples: single-pass and reflective reasoning traces. The single-pass subset includes 1,334 annotated trajectories with an average of 2.7 reasoning steps per trace, representing direct spatial reasoning without correction. The reflective subset includes 392 trajectories with an average of 3.5 reasoning steps, where each trace may include revisions based on prior feedback. On average, 1.2 errors are intentionally injected per reflective sample to simulate self-correction behavior.

Visualizations of response length. Figure 6 compares the evolution of response lengths between our GeoPO and the vanilla GRPO across training steps. GeoPO maintains a stable response length throughout the optimization process while GRPO rapidly collapses to very short outputs (below 50 tokens) within the first 20 steps. These results highlight the effectiveness of our GeoPO in preserving expressive and content-rich responses via step-wise policy optimization.

Prompts for SpatialDreamer-SFT Curation. The prompts for single-pass samples and reflective reasoning samples in the SpatialDreamer-SFT dataset are shown in Figure 9 and Figure 10, respectively.

Evaluation Prompts. The prompts for evaluation on benchmarks of SAT [50], MindCube [67], and VSI-Bench [62] are shown in Figure 11.

Qualitative results of SpatialDreamer. Figure 7 and Figure 8 present the qualitative results of our SpatialDreamer in both simulated and real-world environments. Specifically, Figure 7a illustrates a simulated indoor scenario, where the agent reasons about how to face the window. This example explicitly demonstrates the SpatialDreamer’s ability of *reflective reasoning*, where the agent first moves forward to gather additional spatial cues, then reanalyzes the updated view before making the final directional decision. In contrast, Figure 7b shows a real-world scene inside a train, where SpatialDreamer determines the rotation direction needed to face the door. Together, these examples highlight the generalization of our SpatialDreamer from simulation to real-world settings and its capability to perform multi-step spatial reasoning when necessary.

Table 5. **Key statistics of the SpatialDreamer-SFT dataset.** “Average reasoning steps per trace” represents the average number of interaction rounds. “Injected errors per reflective sample” measures the average number of injected errors per reflective reasoning trace.

Statistics of SpatialDreamer-SFT	Value
Single-pass samples	
Total annotated trajectories	1334
Average reasoning steps per trace	2.7
Reflective samples	
Total annotated trajectories	392
Average reasoning steps per trace	3.5
Injected errors per reflective sample	1.2

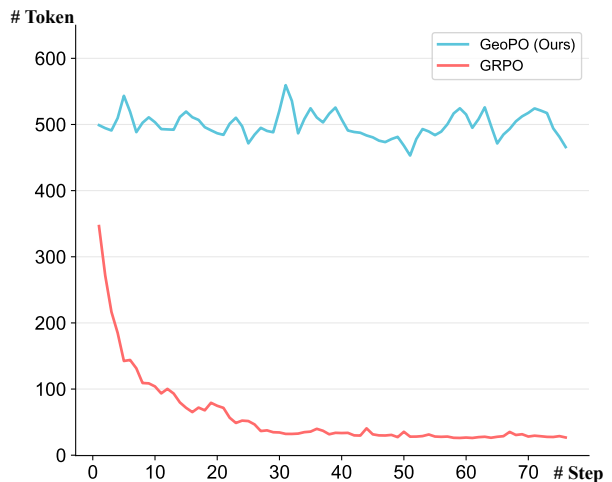


Figure 6. **Comparison of response length** during training. GeoPO maintains stable and informative responses, while GRPO collapses to short outputs.

References

- [1] Anthropic. Claude 3.5 sonnet, 2024. 1
- [2] Anthropic. Claude 4, 2025. 6
- [3] Shuai Bai, Keqin Chen, Xuejing Liu, Jialin Wang, Wenbin Ge, Sibao Song, Kai Dang, Peng Wang, Shijie Wang, Jun Tang, et al. Qwen2. 5-vl technical report. *arXiv preprint arXiv:2502.13923*, 2025. 1, 6, 7
- [4] Christopher Beckham, Martin Weiss, Florian Golemo, Sina Honari, Derek Nowrouzezahrai, and Christopher Pal. Visual question answering from another perspective: Clevr mental rotation tests. *Pattern Recognition*, 136:109209, 2023. 3
- [5] Wenxiao Cai, Iaroslav Ponomarenko, Jianhao Yuan, Xiaoqi Li, Wankou Yang, Hao Dong, and Bo Zhao. Spatialbot: Precise spatial understanding with vision language models. *arXiv preprint arXiv:2406.13642*, 2024. 3
- [6] Zhongang Cai, Yubo Wang, Qingping Sun, Ruisi Wang, Chenyang Gu, Wanqi Yin, Zhiqian Lin, Zhitao Yang, Chen Wei, Xuanke Shi, et al. Has gpt-5 achieved spa-



Figure 7. Qualitative results of our SpatialDreamer.

- tial intelligence? an empirical study. *arXiv preprint arXiv:2508.13142*, 2025. 3
- [7] Fuhao Chang, Shuxin Li, Yabei Li, and Lei He. Vlm-3d: End-to-end vision-language models for open-world 3d perception. *arXiv preprint arXiv:2508.09061*, 2025. 7
- [8] Boyuan Chen, Zhuo Xu, Sean Kirmani, Brain Ichter, Dorsa Sadigh, Leonidas Guibas, and Fei Xia. Spatialvlm: Endowing vision-language models with spatial reasoning capabilities. In *Proceedings of the IEEE/CVF Conference on Computer Vision and Pattern Recognition*, pages 14455–14465, 2024. 2, 6
- [9] Pingyi Chen, Yujing Lou, Shen Cao, Jinhui Guo, Lubin Fan, Yue Wu, Lin Yang, Lizhuang Ma, and Jieping Ye. Sd-vlm: Spatial measuring and understanding with depth-encoded vision-language models. *arXiv preprint arXiv:2509.17664*, 2025. 2, 3
- [10] Xiuwei Chen and Xiaobin Chang. Dynamic residual classifier for class incremental learning. In *Proceedings of the IEEE/CVF International Conference on Computer Vision*, pages 18743–18752, 2023. 6
- [11] Zhe Chen, Weiyun Wang, Yue Cao, Yangzhou Liu, Zhangwei Gao, Erfei Cui, Jinguo Zhu, Shenglong Ye, Hao Tian, Zhaoyang Liu, et al. Expanding performance boundaries of open-source multimodal models with model, data, and test-time scaling. *arXiv preprint arXiv:2412.05271*, 2024. 6
- [12] Zhe Chen, Weiyun Wang, Hao Tian, Shenglong Ye, Zhangwei Gao, Erfei Cui, Wenwen Tong, Kongzhi Hu, Jiapeng Luo, Zheng Ma, et al. How far are we to gpt-4v? closing



Question:

Based on these four images (image 1, 2, 3, and 4) showing the red ball from different viewpoints (front, left, back, and right), with each camera aligned with room walls and partially capturing the surroundings: From the viewpoint presented in image 1, what is to the left of the red ball?

- A. Wall B. Smoking machine
C. Cardboard-covered sliding door D. Window

SpatialDreamer (Ours):

Turn 1

<think>

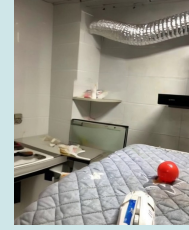
From image 1, the red ball is on a quilt or mattress, and in front of it there is a device with a silver exhaust pipe, likely a kitchen range hood. Image 2 is taken from the red ball's left side, showing a window on that side. Image 3 is from behind the red ball, revealing a sliding door covered with cardboard. Image 4 is from the right side, showing a smooth tiled wall. Starting from image 1 as the initial viewpoint, to determine what is on the left of the red ball, I turn left to inspect the scene.

</think>

<action>

"action": "turn-left", "magnitude": 45

</action>



Mental Imagery of Turn 1

Turn 2

<think>

After turning left, the wall becomes visible, indicating that from the image 1 viewpoint, the left side of the red ball corresponds to the wall.

</think>

<answer> A. Wall </answer>

(a)



Question:

Based on these four images (image 1, 2, 3, and 4) showing the small white table and plastic container from different viewpoints (front, left, back, and right), with each camera aligned with room walls and partially capturing the surroundings: From the viewpoint presented in image 2, what is to the back of the small white table and plastic container?

- A. TV B. Leather loveseat with three seat cushions C. Leather loveseat D. Two single sofas

SpatialDreamer (Ours):

Turn 1

<think>

Image 2 serves as the reference viewpoint, showing the small white table and plastic container in the middle of the room, with a patterned cushion on top. Image 1 shows the front view, facing the TV side, with two sofas visible (one on the left and one on the right). Image 3 shows the left side of the object, where two single sofas are visible along with a chair and small table. Image 4 shows the back view, where the TV and entertainment stand are clearly visible. Thus, from the position and direction of image 2, we need to turn right to determine what is to the back of the small white table and plastic container.

</think>

<action> "action": "turn-right", "magnitude": 90 </action>



Mental Imagery of Turn 1

Turn 2

<think>

After turning right, the TV comes into view. Based on the relative position, it can be determined that from the position and direction of image 2, the TV is located behind. </think>

<answer> A. TV </answer>

(b)

Figure 8. Qualitative results of our SpatialDreamer.

Prompts for SpatialDreamer-SFT (single-pass)

Prompt for tool call

system_prompt = """You are an expert spatial reasoning assistant. Given a spatial reasoning task, suggest ONE tool call that would help verify or explore the spatial relationships.

Available tools:

- generate_svc_image: Generate images by simulating camera movements
- action: "move-forward" (magnitude in meters, e.g., 0.75-2.0)
- action: "turn-left" (magnitude in degrees, e.g., 27-90)
- action: "turn-right" (magnitude in degrees, e.g., 27-90)
- image_index: which image to use as starting point (0 for first original image, or use the index of a previously generated image)

Note: You will see both original images and images generated by previous tool calls. You can use any of them as the starting point.

Respond in JSON format:

```
{
  "action": "turn-right",
  "magnitude": 27,
  "image_index": 0,
  "reasoning": "Turn right from image 1 to verify the object's position on the right side"
}
```

first tool call

user_prompt = f"""

Task Context: {task}

Initial Reasoning: {init_reason}

You have {len(image_paths)} original image(s) available.

Please suggest the FIRST tool call that would help explore the spatial relationships.

"""

second tool call

user_prompt = f"""

Task Context: {task}

Initial Reasoning: {init_reason}

Previous tool execution history:

Step {idx}:

- Reasoning: {prev_step.get('reasoning', 'N/A')}\n"
- Tool Call: {json.dumps(prev_step.get('tool_call', {}), ensure_ascii=False)}\n"
- Tool Response: {prev_step.get('tool_response', 'N/A')} <image>\n"

You now have {len(image_paths)} image(s) available "

(including original images and images generated by previous tool calls).

You can use any of them as the starting point for the next tool call.

Please suggest the SECOND tool call based on the previous observations and available images.

"""

Prompt for answer generation

system_prompt = """You are an expert spatial analyst. Based on the task, initial reasoning, and tool execution results, provide a final comprehensive reasoning and answer. You will see both original images and images generated by tool calls. Use all available visual information to make your final assessment."""

user_prompt = f"""Task Context: {human_prompt}

Initial Reasoning: {think_text}

Tool Execution History: {chr(10).join(tool_history)}{image_info}

Please synthesize all the information above (including all available images) and provide your final reasoning and answer. Format your response strictly as: <think>Your comprehensive reasoning here</think><answer>Your final answer here</answer>"""

Figure 9. Prompts for generating single-pass reasoning samples in SpatialDreamer-SFT dataset.

- the gap to commercial multimodal models with open-source suites. *arXiv preprint arXiv:2404.16821*, 2024. 7
- [13] Zhangquan Chen, Manyuan Zhang, Xinlei Yu, Xufang Luo, Mingze Sun, Zihao Pan, Yan Feng, Peng Pei, Xunliang Cai, and Ruqi Huang. Think with 3d: Geometric imagination grounded spatial reasoning from limited views. *arXiv preprint arXiv:2510.18632*, 2025. 3, 6
- [14] Erik Daxberger, Nina Wenzel, David Griffiths, Haiming Gang, Justin Lazarow, Gefen Kohavi, Kai Kang, Marcin Eichner, Yinfei Yang, Afshin Dehghan, et al. Mm-spatial: Exploring 3d spatial understanding in multimodal llms. In *Proceedings of the IEEE/CVF International Conference on Computer Vision*, pages 7395–7408, 2025. 3
- [15] Paola Del Sette, Markus Bindemann, and Heather J Ferguson. Visual perspective-taking in complex natural scenes. *Quarterly Journal of Experimental Psychology*, 75(8):1541–1551, 2022. 3
- [16] Zhiwen Fan, Jian Zhang, Renjie Li, Junge Zhang, Runjin Chen, Hezhen Hu, Kevin Wang, Huaizhi Qu, Dilin Wang, Zhicheng Yan, et al. Vlm-3r: Vision-language models augmented with instruction-aligned 3d reconstruction. *arXiv preprint arXiv:2505.20279*, 2025. 2, 3
- [17] Huang Fang, Mengxi Zhang, Heng Dong, Wei Li, Zixuan Wang, Qifeng Zhang, Xueyun Tian, Yucheng Hu, and Hang Li. Robix: A unified model for robot interaction, reasoning and planning. *arXiv preprint arXiv:2509.01106*, 2025. 6
- [18] Kaituo Feng, Kaixiong Gong, Bohao Li, Zonghao Guo, Yibing Wang, Tianshuo Peng, Junfei Wu, Xiaoying Zhang, Benyou Wang, and Xiangyu Yue. Video-r1: Reinforcing video reasoning in mllms. *arXiv preprint arXiv:2503.21776*, 2025. 7
- [19] Ronald A Finke. *Principles of mental imagery*. The MIT Press, 1989. 3
- [20] Rao Fu, Jingyu Liu, Xilun Chen, Yixin Nie, and Wenhan Xiong. Scene-llm: Extending language model for 3d visual understanding and reasoning. *arXiv preprint arXiv:2403.11401*, 2024. 3
- [21] Howard Gardner. *Frames of mind: The theory of multiple intelligences*. Basic books, 2011. 1
- [22] Mohsen Gholami, Ahmad Rezaei, Zhou Weimin, Sitong Mao, Shunbo Zhou, Yong Zhang, and Mohammad Akbari. Spatial reasoning with vision-language models in ego-centric multi-view scenes. *arXiv preprint arXiv:2509.06266*, 2025. 3, 6
- [23] Daya Guo, Dejian Yang, Haowei Zhang, Junxiao Song, Ruoyu Zhang, Runxin Xu, Qihao Zhu, Shirong Ma, Peiyi Wang, Xiao Bi, et al. Deepseek-r1: Incentivizing reasoning capability in llms via reinforcement learning. *arXiv preprint arXiv:2501.12948*, 2025. 2, 3, 4
- [24] Yining Hong, Haoyu Zhen, Peihao Chen, Shuhong Zheng, Yilun Du, Zhenfang Chen, and Chuang Gan. 3d-llm: Injecting the 3d world into large language models. *Advances in Neural Information Processing Systems*, 36:20482–20494, 2023. 3
- [25] Coleman Hooper, Sehoon Kim, Suhong Moon, Kerem Dilmen, Monishwaran Maheswaran, Nicholas Lee, Michael W Mahoney, Sophia Shao, Kurt Keutzer, and Amir Gholami. Ets: Efficient tree search for inference-time scaling. *arXiv preprint arXiv:2502.13575*, 2025. 3
- [26] Zhenyu Hou, Ziniu Hu, Yujiang Li, Rui Lu, Jie Tang, and Yuxiao Dong. Treerl: Llm reinforcement learning with on-policy tree search. *arXiv preprint arXiv:2506.11902*, 2025. 3
- [27] Xiaohu Huang, Jingjing Wu, Qunyi Xie, and Kai Han. Mllms need 3d-aware representation supervision for scene understanding. *arXiv preprint arXiv:2506.01946*, 2025. 2, 3
- [28] Aaron Jaech, Adam Kalai, Adam Lerer, Adam Richardson, Ahmed El-Kishky, Aiden Low, Alec Helyar, Aleksander Madry, Alex Beutel, Alex Carney, et al. Openai o1 system card. *arXiv preprint arXiv:2412.16720*, 2024. 3, 6
- [29] Yuheng Ji, Huajie Tan, Jiayu Shi, Xiaoshuai Hao, Yuan Zhang, Hengyuan Zhang, Pengwei Wang, Mengdi Zhao, Yao Mu, Pengju An, et al. Robobrain: A unified brain model for robotic manipulation from abstract to concrete. In *Proceedings of the Computer Vision and Pattern Recognition Conference*, pages 1724–1734, 2025. 6
- [30] Dongfu Jiang, Xuan He, Huaye Zeng, Cong Wei, Max Ku, Qian Liu, and Wenhui Chen. Mantis: Interleaved multi-image instruction tuning. *arXiv preprint arXiv:2405.01483*, 2024. 6
- [31] Eric Kolve, Roozbeh Mottaghi, Winson Han, Eli VanderBilt, Luca Weihs, Alvaro Herrasti, Matt Deitke, Kiana Ehsani, Daniel Gordon, Yuke Zhu, et al. Ai2-thor: An interactive 3d environment for visual ai. *arXiv preprint arXiv:1712.05474*, 2017. 5
- [32] Phillip Y Lee, Jihyeon Je, Chanho Park, Mikaela Angelina Uy, Leonidas Guibas, and Minhyuk Sung. Perspective-aware reasoning in vision-language models via mental imagery simulation. *arXiv preprint arXiv:2504.17207*, 2025. 3
- [33] Bo Li, Kaichen Zhang, Hao Zhang, Dong Guo, Renrui Zhang, Feng Li, Yuanhan Zhang, Ziwei Liu, and Chunyuan Li. Llava-next: Stronger llms supercharge multimodal capabilities in the wild, 2024. 7
- [34] Bo Li, Yuanhan Zhang, Dong Guo, Renrui Zhang, Feng Li, Hao Zhang, Kaichen Zhang, Yanwei Li, Ziwei Liu, and Chunyuan Li. Llava-onevision: Easy visual task transfer. *arXiv preprint arXiv:2408.03326*, 2024. 6, 7
- [35] Lei Li, Yuancheng Wei, Zhihui Xie, Xuqing Yang, Yifan Song, Peiyi Wang, Chenxin An, Tianyu Liu, Sujian Li, Bill Yuchen Lin, et al. V1-rewardbench: A challenging benchmark for vision-language generative reward models. In *Proceedings of the Computer Vision and Pattern Recognition Conference*, pages 24657–24668, 2025. 3
- [36] Yizhi Li, Qingshui Gu, Zhoufutu Wen, Ziniu Li, Tian-shun Xing, Shuyue Guo, Tianyu Zheng, Xin Zhou, Xingwei Qu, Wangchunshu Zhou, et al. Treepo: Bridging the gap of policy optimization and efficacy and inference efficiency with heuristic tree-based modeling. *arXiv preprint arXiv:2508.17445*, 2025. 3
- [37] Zhenyi Liao, Qingsong Xie, Yanhao Zhang, Zijian Kong, Haonan Lu, Zhenyu Yang, and Zhijie Deng. Improved visual-spatial reasoning via r1-zero-like training. *arXiv preprint arXiv:2504.00883*, 2025. 2, 3, 7

- [38] Hunter Lightman, Vineet Kosaraju, Yuri Burda, Harrison Edwards, Bowen Baker, Teddy Lee, Jan Leike, John Schulman, Ilya Sutskever, and Karl Cobbe. Let’s verify step by step. In *The Twelfth International Conference on Learning Representations*, 2023. 3
- [39] Haotian Liu, Chunyuan Li, Qingyang Wu, and Yong Jae Lee. Visual instruction tuning. *Advances in neural information processing systems*, 36, 2024. 6
- [40] Yang Liu, Ming Ma, Xiaomin Yu, Pengxiang Ding, Han Zhao, Mingyang Sun, Siteng Huang, and Donglin Wang. Ssr: Enhancing depth perception in vision-language models via rationale-guided spatial reasoning. *arXiv preprint arXiv:2505.12448*, 2025. 3
- [41] Haoyu Lu, Wen Liu, Bo Zhang, Bingxuan Wang, Kai Dong, Bo Liu, Jingxiang Sun, Tongzheng Ren, Zhuoshu Li, Hao Yang, et al. Deepseek-vl: towards real-world vision-language understanding. *arXiv preprint arXiv:2403.05525*, 2024. 6
- [42] Wufei Ma, Haoyu Chen, Guofeng Zhang, Yu-Cheng Chou, Celso M de Melo, and Alan Yuille. 3dsrbench: A comprehensive 3d spatial reasoning benchmark. *arXiv preprint arXiv:2412.07825*, 2024. 3
- [43] Nora S Newcombe and Janellen Huttenlocher. Development of spatial cognition. *Handbook of child psychology*, 2, 2007. 1
- [44] OpenAI. Gpt-4v(ision) system card. <https://api.semanticscholar.org/CorpusID:263218031>, 2023. 6
- [45] OpenAI. Hello gpt-4o. *OpenAI Blog*, 2024. 1, 2, 6, 7
- [46] OpenAI. Gpt-4.1 technical overview. <https://openai.com/index/gpt-4-1/>, 2024. 6
- [47] Kun Ouyang, Yuanxin Liu, Haoning Wu, Yi Liu, Hao Zhou, Jie Zhou, Fandong Meng, and Xu Sun. Spacer: Reinforcing mllms in video spatial reasoning. *arXiv preprint arXiv:2504.01805*, 2025. 3, 7
- [48] Long Ouyang, Jeffrey Wu, Xu Jiang, Diogo Almeida, Carroll Wainwright, Pamela Mishkin, Chong Zhang, Sandhini Agarwal, Katarina Slama, Alex Ray, et al. Training language models to follow instructions with human feedback. *Advances in neural information processing systems*, 35:27730–27744, 2022. 3
- [49] Zhangyang Qi, Zhixiong Zhang, Ye Fang, Jiaqi Wang, and Hengshuang Zhao. Gpt4scene: Understand 3d scenes from videos with vision-language models. *arXiv preprint arXiv:2501.01428*, 2025. 3
- [50] Arijit Ray, Jiafei Duan, Ellis Brown, Reuben Tan, Dina Bashkirova, Rose Hendrix, Kiana Ehsani, Aniruddha Kembhavi, Bryan A Plummer, Ranjay Krishna, et al. Sat: Dynamic spatial aptitude training for multimodal language models. *arXiv preprint arXiv:2412.07755*, 2024. 2, 3, 5, 6, 9
- [51] Ray Project. Ray: A unified framework for scaling ai and python applications. <https://github.com/ray-project/ray>, 2024. 6
- [52] Machel Reid, Nikolay Savinov, Denis Teplyashin, Dmitry Lepikhin, Timothy Lillicrap, Jean-baptiste Alayrac, Radu Soricut, Angeliki Lazaridou, Orhan Firat, Julian Schrittwieser, et al. Gemini 1.5: Unlocking multimodal understanding across millions of tokens of context. *arXiv preprint arXiv:2403.05530*, 2024. 6
- [53] Jiacheng Ruan, Wenzhen Yuan, Xian Gao, Ye Guo, Daoxin Zhang, Zhe Xu, Yao Hu, Ting Liu, and Yuzhuo Fu. Vlrbench: A comprehensive and challenging benchmark for vision-language reward models. *arXiv preprint arXiv:2503.07478*, 2025. 3
- [54] Guangming Sheng, Chi Zhang, Zilingfeng Ye, Xibin Wu, Wang Zhang, Ru Zhang, Yanghua Peng, Haibin Lin, and Chuan Wu. Hybridflow: A flexible and efficient rlhf framework. *arXiv preprint arXiv: 2409.19256*, 2024. 6
- [55] Joar Skalse, Nikolaus Howe, Dmitrii Krashenninnikov, and David Krueger. Defining and characterizing reward gaming. *Advances in Neural Information Processing Systems*, 35:9460–9471, 2022. 3
- [56] Charlie Snell, Jaehoon Lee, Kelvin Xu, and Aviral Kumar. Scaling llm test-time compute optimally can be more effective than scaling model parameters. *arXiv preprint arXiv:2408.03314*, 2024. 2, 3
- [57] Gemini Team, Petko Georgiev, Ving Ian Lei, Ryan Burnell, Libin Bai, Anmol Gulati, Garrett Tanzer, Damien Vincent, Zhufeng Pan, Shibo Wang, et al. Gemini 1.5: Unlocking multimodal understanding across millions of tokens of context. *arXiv preprint arXiv:2403.05530*, 2024. 7
- [58] Jianyuan Wang, Minghao Chen, Nikita Karaev, Andrea Vedaldi, Christian Rupprecht, and David Novotny. Vggt: Visual geometry grounded transformer. In *Proceedings of the Computer Vision and Pattern Recognition Conference*, pages 5294–5306, 2025. 3, 7
- [59] Qianqian Wang, Yifei Zhang, Aleksander Holynski, Alexei A Efros, and Angjoo Kanazawa. Continuous 3d perception model with persistent state. In *Proceedings of the Computer Vision and Pattern Recognition Conference*, pages 10510–10522, 2025. 3, 7
- [60] Diankun Wu, Fangfu Liu, Yi-Hsin Hung, and Yueqi Duan. Spatial-mllm: Boosting mllm capabilities in visual-based spatial intelligence. *arXiv preprint arXiv:2505.23747*, 2025. 6
- [61] Wenrui Xu, Dalin Lyu, Weihang Wang, Jie Feng, Chen Gao, and Yong Li. Defining and evaluating visual language models’ basic spatial abilities: A perspective from psychometrics. *arXiv preprint arXiv:2502.11859*, 2025. 3
- [62] Jihan Yang, Shusheng Yang, Anjali W Gupta, Rilyn Han, Li Fei-Fei, and Saining Xie. Thinking in space: How multimodal large language models see, remember, and recall spaces. In *Proceedings of the Computer Vision and Pattern Recognition Conference*, pages 10632–10643, 2025. 2, 5, 9
- [63] Yuncong Yang, Jiageng Liu, Zheyuan Zhang, Siyuan Zhou, Reuben Tan, Jianwei Yang, Yilun Du, and Chuang Gan. Mindjourney: Test-time scaling with world models for spatial reasoning. *arXiv preprint arXiv:2507.12508*, 2025. 2, 3, 6
- [64] Zhicheng Yang, Zhijiang Guo, Yinya Huang, Xiaodan Liang, Yiwei Wang, and Jing Tang. Treerpo: Tree relative policy optimization. *arXiv preprint arXiv:2506.05183*, 2025. 3
- [65] Zeyuan Yang, Xueyang Yu, Delin Chen, Maohao Shen, and Chuang Gan. Machine mental imagery: Empower multi-

- modal reasoning with latent visual tokens. *arXiv preprint arXiv:2506.17218*, 2025. 3
- [66] Shunyu Yao, Dian Yu, Jeffrey Zhao, Izhak Shafran, Tom Griffiths, Yuan Cao, and Karthik Narasimhan. Tree of thoughts: Deliberate problem solving with large language models. *Advances in neural information processing systems*, 36:11809–11822, 2023. 3
- [67] Baiqiao Yin, Qineng Wang, Pingyue Zhang, Jianshu Zhang, Kangrui Wang, Zihan Wang, Jieyu Zhang, Keshigeyan Chandrasegaran, Han Liu, Ranjay Krishna, et al. Spatial mental modeling from limited views. In *Structural Priors for Vision Workshop at ICCV’25*, 2025. 2, 3, 5, 6, 8, 9
- [68] Qiyang Yu, Zheng Zhang, Ruofei Zhu, Yufeng Yuan, Xiaochen Zuo, Yu Yue, Weinan Dai, Tiantian Fan, Gao-hong Liu, Lingjun Liu, et al. Dapo: An open-source llm reinforcement learning system at scale. *arXiv preprint arXiv:2503.14476*, 2025. 2, 3
- [69] Wentao Yuan, Jiafei Duan, Valts Blukis, Wilbert Pumacay, Ranjay Krishna, Adithyavairavan Murali, Arsalan Mousavian, and Dieter Fox. Robopoint: A vision-language model for spatial affordance prediction for robotics. *arXiv preprint arXiv:2406.10721*, 2024. 6
- [70] Yu Yue, Yufeng Yuan, Qiyang Yu, Xiaochen Zuo, Ruofei Zhu, Wenyuan Xu, Jiaze Chen, Chengyi Wang, TianTian Fan, Zhengyin Du, et al. Vapo: Efficient and reliable reinforcement learning for advanced reasoning tasks. *arXiv preprint arXiv:2504.05118*, 2025. 2, 3
- [71] Jirong Zha, Yuxuan Fan, Xiao Yang, Chen Gao, and Xinlei Chen. How to enable llm with 3d capacity? a survey of spatial reasoning in llm. *arXiv preprint arXiv:2504.05786*, 2025. 3
- [72] Bolin Zhang, Jiahao Wang, Qianlong Du, Jiajun Zhang, Zhiying Tu, and Dianhui Chu. A survey on data selection for llm instruction tuning. *Journal of Artificial Intelligence Research*, 83, 2025. 5
- [73] Jiawei Zhang, Chejian Xu, and Bo Li. Chatscene: Knowledge-enabled safety-critical scenario generation for autonomous vehicles. In *Proceedings of the IEEE/CVF Conference on Computer Vision and Pattern Recognition*, pages 15459–15469, 2024. 3
- [74] Jiahui Zhang, Yurui Chen, Yanpeng Zhou, Yueming Xu, Ze Huang, Jilin Mei, Junhui Chen, Yu-Jie Yuan, Xinyue Cai, Guowei Huang, et al. From flatland to space: Teaching vision-language models to perceive and reason in 3d. *arXiv preprint arXiv:2503.22976*, 2025. 2, 3, 5, 7
- [75] Peiyuan Zhang, Kaichen Zhang, Bo Li, Guangtao Zeng, Jingkan Yang, Yuanhan Zhang, Ziyue Wang, Haoran Tan, Chunyuan Li, and Ziwei Liu. Long context transfer from language to vision. *arXiv preprint arXiv:2406.16852*, 2024. 6
- [76] Wenyu Zhang, Wei En Ng, Lixin Ma, Yuwen Wang, Junqi Zhao, Allison Koenecke, Boyang Li, and Lu Wang. Sphere: Unveiling spatial blind spots in vision-language models through hierarchical evaluation. *arXiv preprint arXiv:2412.12693*, 2024. 3
- [77] Weichen Zhang, Zile Zhou, Zhiheng Zheng, Chen Gao, Jin-qiang Cui, Yong Li, Xinlei Chen, and Xiao-Ping Zhang. Open3dvqa: A benchmark for comprehensive spatial reasoning with multimodal large language model in open space. *arXiv preprint arXiv:2503.11094*, 2025. 3
- [78] Yuanhan Zhang, Jinming Wu, Wei Li, Bo Li, Zejun Ma, Ziwei Liu, and Chunyuan Li. Video instruction tuning with synthetic data. *arXiv preprint arXiv:2410.02713*, 2024. 5, 6
- [79] Zheyuan Zhang, Fengyuan Hu, Jayjun Lee, Freda Shi, Parisa Kordjamshidi, Joyce Chai, and Ziqiao Ma. Do vision-language models represent space and how? evaluating spatial frame of reference under ambiguities. *arXiv preprint arXiv:2410.17385*, 2024. 2
- [80] Hao Zhao, Maksym Andriushchenko, Francesco Croce, and Nicolas Flammarion. Long is more for alignment: A simple but tough-to-beat baseline for instruction fine-tuning. *arXiv preprint arXiv:2402.04833*, 2024. 5
- [81] Duo Zheng, Shijia Huang, Yanyang Li, and Liwei Wang. Learning from videos for 3d world: Enhancing mllms with 3d vision geometry priors. *arXiv preprint arXiv:2505.24625*, 2025. 2, 3, 5, 7
- [82] Jialun Zhong, Wei Shen, Yanzeng Li, Songyang Gao, Hua Lu, Yicheng Chen, Yang Zhang, Wei Zhou, Jinjie Gu, and Lei Zou. A comprehensive survey of reward models: Taxonomy, applications, challenges, and future. *arXiv preprint arXiv:2504.12328*, 2025. 3
- [83] Chunting Zhou, Pengfei Liu, Puxin Xu, Srinivasan Iyer, Jiao Sun, Yuning Mao, Xuezhe Ma, Avia Efrat, Ping Yu, Lili Yu, et al. Lima: Less is more for alignment. *Advances in Neural Information Processing Systems*, 36:55006–55021, 2023. 5
- [84] Jensen Zhou, Hang Gao, Vikram Voleti, Aaryaman Vasishta, Chun-Han Yao, Mark Boss, Philip Torr, Christian Rupprecht, and Varun Jampani. Stable virtual camera: Generative view synthesis with diffusion models. *arXiv preprint arXiv:2503.14489*, 2025. 1, 2, 3, 6
- [85] Jinguo Zhu, Weiyun Wang, Zhe Chen, Zhaoyang Liu, Shenglong Ye, Lixin Gu, Yuchen Duan, Hao Tian, Weijie Su, Jie Shao, et al. Internvl3: Exploring advanced training and test-time recipes for open-source multimodal models. *arXiv preprint arXiv:2504.10479*, 2025. 6

Prompts for SpatialDreamer-SFT (Reflective Reasoning)

Prompt for tool call

system_prompt = ""You are an expert spatial reasoning assistant.

Available tools:

- generate_svc_image: Generate images by simulating camera movements
- action: "move-forward" (magnitude in meters, e.g., 0.75-2.0)
- action: "turn-left" (magnitude in degrees, e.g., 27-90)
- action: "turn-right" (magnitude in degrees, e.g., 27-90)
- image_index: which image to use as starting point (0 for first original image, or use the index of a previously generated image)

Note: You will see both original images and images generated by previous tool calls. You can use any of them as the starting point.

Respond in JSON format:

```
{
  "action": "turn-right",
  "magnitude": 27,
  "image_index": 0,
  "reasoning": "Turn right from image 1 to verify the object's position on the right side"
}
```

first tool call

user_prompt = f""

Task Context: {task}

Initial Reasoning: {init_reason}

You have {len(image_paths)} original image(s) available.

Important constraint for this step:

Deliberately choose an action that is unlikely to help answer the task (i.e., an uninformative or irrelevant camera move), while still being a valid tool call.

Please suggest the FIRST tool call. It should:

Be valid syntactically.

Be spatially plausible but unhelpful for clarifying the task.

Include concise reasoning explaining why this action is (ironically) not helpful.

""

second tool call

user_prompt = f""

Task Context: {task}

Initial Reasoning: {init_reason}

Previous tool execution history:

Step {idx}:

- Reasoning: {prev_step.get('reasoning', 'N/A')}\n"
- Tool Call: {json.dumps(prev_step.get('tool_call', {}), ensure_ascii=False)}\n"
- Tool Response: {prev_step.get('tool_response', 'N/A')} <image>\n"

You now have {len(image_paths)} image(s) available "

(including original images and images generated by previous tool calls).

You can use any of them as the starting point for the next tool call.

Your objective for this step:

Recognize that the first action was unhelpful.

Provide a corrective, task-relevant action that maximizes information gain about the spatial relationships in question.

Justify how this new action addresses the deficiency of the first action and leverages available images.

Please suggest the SECOND tool call.

""

Prompt for answer generation

system_prompt = ""You are an expert spatial analyst. Based on the task, initial reasoning, and tool execution results, provide a final comprehensive reasoning and answer. You will see both original images and images generated by tool calls. Use all available visual information to make your final assessment.""

user_prompt = f""Task Context: {human_prompt}

Initial Reasoning: {think_text}

Tool Execution History: {chr(10).join(tool_history)}{image_info}

Please synthesize all the information above (including all available images) and provide your final reasoning and answer.

Format your response strictly as: <think>Your comprehensive reasoning here</think><answer>Your final answer here</answer>""

Figure 10. Prompts for generating reflective reasoning samples in SpatialDreamer-SFT dataset.

Evaluation Prompt
<pre>f""< im_start >system You are a helpful assistant. # Tools You may call one or more functions to assist with the user query. You are provided with function signatures within <tools></tools> XML tags: <tools> {"type": "function", "function": {"name": "image_generator", "description": "A tool for generating image by taking actions in 3D space using the SVC (Stable Virtual Camera) world model.", "parameters": {"type": "object", "properties": {"action": {"type": "string", "description": "The action to take in the 3D space. Must be one of: 'move-forward' (move camera forward), 'turn-left' (rotate camera left), 'turn-right' (rotate camera right)", "enum": ["move-forward", "turn-left", "turn-right"]}, "magnitude": {"type": "number", "description": "The magnitude of the action. For 'move-forward', this is the distance in meters (e.g., 0.75). For 'turn-left' or 'turn-right', this is the angle in degrees (e.g., 27)"}, "image_index": {"type": "integer", "description": "The index of the image to generate. The first image is 0."}}, "required": ["action", "magnitude", "image_index"]}}} </tools> For each function call, return a json object with function name and arguments within <tool_call></tool_call> XML tags: <tool_call> {"name": <function-name>, "arguments": <args-json-object>} </tool_call>< im_end > < im_start >user Answer the given question. You must conduct reasoning inside <think> and </think> first every time you get new information. After reasoning, if you find you lack some knowledge, you can call the image generator by <tool_call> query </tool_call> to explore the 3D space by taking actions like moving forward or turning and it will return the generated image based on your selected image and action between <tool_response> and </tool_response>. You can call the tool as many times as your want. If you find no further external knowledge needed, you can directly provide the answer inside <answer> and </answer>, without detailed illustrations. For example, <answer> Beijing </answer>. Question: {Task} < im_end > < im_start >assistant """</pre>

Figure 11. Prompts for evaluation on SAT, MindCube, and VSI-Bench.